Int. J. Electrochem. Sci., 14 **(2019)** 9239 – 9254, doi: 10.20964/2019.09.84

International Journal of
ELECTROCHEMICAL
SCIENCE
www.electrochemsci.org

Investigation of the Material Removal Mechanism in Electrochemical Discharge Drilling Using a High-Speed Rotating Helical Tool-Electrode

Xianchun Shi, Shaofu Huang[*]*, Long Wang*

School of Mechanical Engineering, Anhui University of Science and Technology, 168 Taifeng Road, Anhui, Huainan 232001, China.
[*]E-mail: huangshaofu1974@163.com

Received: 24 May 2019 / *Accepted:* 17 July 2019 / *Published:* 5 August 2019

The electrochemical discharge machining (ECDM) process is an effective way for non-traditional machining technology to machine micro-pits on conductive, non-conductive, hard and brittle materials, including glass, quartz, stainless steel and so on. In this paper, many experiments are discussed that investigate the material removal mechanism during the electrochemical discharge drilling (ECDD) process. The present research mainly discusses the effect of tool-electrode rotational speed on gas film formation, the electric discharge phenomenon, machining current, diameter of the micro-pit, machining depth of the micro-pit and material removal rate (MRR) of the work-piece. The experimental results demonstrate that when the tool-electrode is in a high-speed rotational state, removal of the work-piece material is due to the synergy of electrochemical corrosion and electric spark discharge. By contrast, when the tool-electrode is in a stationary state, the removal of the work-piece material is mainly by electrochemical corrosion. In addition, the experimental results show that the surface of the gas film becomes denser and more uniform with the increase in tool-electrode rotational speed and that the MRR is significantly increased. Eventually, a series of micro-pits are successfully fabricated by this high-speed rotating ECDD process.

Keywords: Electrochemical discharge machining (ECDM); Electrochemical discharge drilling (ECDD); Micro-pit; Tool-electrode rotational speed; the machining current, Material removal rate (MRR).

1. INTRODUCTION

With the rapid development of micro electro-mechanical systems (MEMS) technology, electrochemical discharge machining (ECDM) has received extensive attention in the field of micro-fabrication [1-3]. The ECDM process is a kind of non-traditional machining technology based on spark discharge effects and can process conductive and non-conductive materials. The processing technology

can effectively machine difficult-to-cut materials, such as glass, metal matrix composites, ceramics, quartz and stainless steel [4-7]. Compared with laser machining, ultrasonic machining, abrasive water jet and chemical corrosion, ECDM has the advantages of a high processing efficiency, simple installation, low cost and good processing flexibility [8]. Therefore, the electrochemical discharge machining process has broad prospects for development.

The ECDM process was initially proposed by Kurafuji in 1968 and applied to drill micro-holes on a glass material [9]. Subsequently, this machining process has received extensive attention in the field of micro-fabrication. Many researchers have conducted in-depth scientific research on the material removal mechanism and machining parameters for electrochemical discharge material removal. In the academic community, ECDM is referred to by different names. Cook et al. called ECDM discharge machining of non-conductors [10]. Tandon et al. called ECDM electrochemical spark machining (ECSM) [11]. Wüthrich et al. called ECDM electrochemical arc machining (ECAM) [12]. Langen et al. called ECDM spark assisted chemical engraving (SACE) [13]. In recent years, the academic community has generally referred to this process as ECDM [14-17]. In this paper, we used the term ECDM.

Basak et al. developed a simplified theoretical model for the ECDM process to predict the minimum voltage needed for spark discharge and the critical current for the machining process, which provided a theoretical basis for further investigating the material removal mechanism of the ECDM process [18]. During the process of generating electrochemical discharge drilling-holes, the rotational speed of the tool-electrode is an important parameter that influences the machining quality [19]. Zheng et al. studied the effects of different tool-electrode rotational speeds (from 200 to 2000 rpm) on the machining quality of electrochemical discharge micro-milling. They found that the groove width decreased as the rotational speed of tool-electrode increased. The possible reason for this decrease was that the thickness of the gas film becomes thinner and more homogeneous with the increasing tool-electrode rotational speed. In addition, they also found that the rotational speed of the tool-electrode did not have a conspicuous effect on the machining depth [20]. Wüthrich et al. reported that the material removal rate and the circularity of the machined micro-holes were improved by a rotational tool-electrode. They divided the effects of the tool-electrode rotational speed on the machining efficiency into two categories: at a lower rotational speed (less than 25 rpm), the machining efficiency increased as the rotational speed of the tool-electrode increased; at a higher rotational speed (more than 25 rpm), the machining efficiency decreased as the rotational speed of the tool-electrode increased [12]. Gautam et al. carried out a series of experiments to investigate the influence of the tool-electrode rotational speed on the machining efficiency. Their experimental results showed that the machining efficiency was influenced by the effects of the tool-electrode rotational speed on the stability of electrochemical discharge in the process of machining [21]. However, some progress has been made given that these investigations were mainly based on a low rotational speed of the tool-electrode. Huang et al. investigated the effects of a high-speed rotating tool-electrode on the machining parameters of micro-holes during the process of electrochemical discharge machining. In the experiment, tap water was used as the electrolyte, a tungsten carbide helical tool-electrode was used as the tool-electrode, and the maximum rotational speed of the tool-electrode was set at 42,000 rpm. Their experimental results demonstrated that the material removal rate for a work-piece was improved, the surface roughness of the micro-holes was decreased, and the stray current corrosions of the entrance and exit of the micro-holes

were reduced by electrochemical discharge machining with a high-speed rotating helical tool-electrode [22]. Huang et al. established an empirical mathematical model for tool-electrode wear using the experimental results of micro-hole processing on stainless steel by ECDM. They found that the parameters (from large to small) of the tool-electrode wear obtained from the empirical mathematical model were the machining voltage, the rotational speed of the tool-electrode, and the diameter of the tool-electrode, which provided experience for further study of the wear rate of the tool-electrode [23]. Fang et al. utilized a rotating helical tool-electrode to improve the machining performance of wire-electrochemical micro-machining. In the experiment, the maximum feed speed (2 and 6 μm/s) of the tool-electrode was obtained, which rotated at different rotational speeds (5,000 and 20,000 rpm). They found that the maximum feed speed of the tool-electrode increased with the rotational speed of the tool-electrode [24]. Liu et al. showed the effect of the spindle speed on the side gap of a series of kerfs machined in a glass work-piece. Their experiments showed that the machining side gap decreased with the increasing spindle speed when the spindle speed rotated at 3,000-12,000 rpm. When the spindle speed was 15,000 rpm, the machining tool-electrode broke. They also found that a spindle speed of 3,000 rpm increased spark discharge compared to a spindle speed of 9000 rpm, possibly because it was more difficult to form a stable gas film at higher tool-electrode rotational speeds [25].

Nevertheless, the electric discharge performance and the material removal mechanism of work-piece materials have been poorly reported in the literature. In this paper, a high-speed rotating helical tool-electrode is employed in the experimental set-up of the ECDD process. This paper mainly aims to investigate the material removal mechanism during the practical machining process.

In the experiments performed in this study, the effects of the tool-electrode rotational speed on the gas film formation, the electric discharge phenomenon, the machining current, the diameter of micro-pit, the machining depth of the micro-pit, and the material removal rate (MRR) of the work-piece are studied. The experimental results show that when the tool-electrode is in a high-speed rotational state, the removal of the work-piece material is due to the synergy of electrochemical corrosion and electric spark discharge. In addition, the experimental results also demonstrate that the surface of the gas film becomes denser and more uniform with the increase in the tool-electrode rotational speed and that the MRR is significantly enhanced.

2. ECDD PRINCIPLE

The ECDD process is a kind of hybrid processing method. This processing method is built on the basis of both the EDM and the ECM processes, which can be used to machine micro-pits on conductive and non-conductive materials. Xu et al. performed tube electrode high-speed electrochemical discharge drilling of micro-holes using low-resistivity deionized water as the working-fluid to achieve a high machining efficiency and surface quality. During the course of their experimental research, the tube electrode rotation was 100 rpm [26]. However, by contrast, we present a machining method for micro-pitting using a high-speed rotating tungsten carbide helical tool-electrode; the centre of the tool-electrode is solid. More importantly, the rotational speed of the tool-electrode is 3,600 rpm to 18,000rpm. Thus, during the electrochemical discharge drilling process, the material removal mechanism is very

researchable. Because our method uses a tungsten carbide helical electrode as the tool-electrode and tap water of extremely low conductivity as the electrolyte, the processing results for the work-piece surface are induced by the synergy of electrochemical corrosion and electric spark discharge. The removal mechanism for the work-piece material in this hybrid machining process mainly depends on gas film formation and the electric spark discharge generated. The schematic diagram of the ECDD principle is illustrated in Fig 1. As shown, the whole ECDD process can be divided into five stages. (i) Bubble generation comes from two parts: (a) hydrogen and oxygen are generated as by-products of the electrochemical reactions between the tool-electrode and the electrolyte, and (b) since a large amount of thermal energy is released during the electrolysis process, the electrolyte near the surface of the tool-electrode is evaporated to produce water vapour bubbles, as shown in Fig 1 (a). (ii) These bubbles begin to accumulate on the surface of the tool-electrode under centrifugal force, as shown in Fig 1 (b). (iii) The bubbles that accumulate on the surface of the tool-electrode form a gas film, which is a mixture of steam, hydrogen and oxygen, as shown in Fig 1 (c). (iv) When the applied machining voltage reaches the critical machining voltage, the gas film is instantly broken-down, and a cluster of electric sparks is generated, as shown in Fig 1 (d). (v) The thermal energy released from the electric spark discharge is used to remove the work-piece material, and a micro-pit is thermally etched on its surface, as shown in Fig 1 (e).

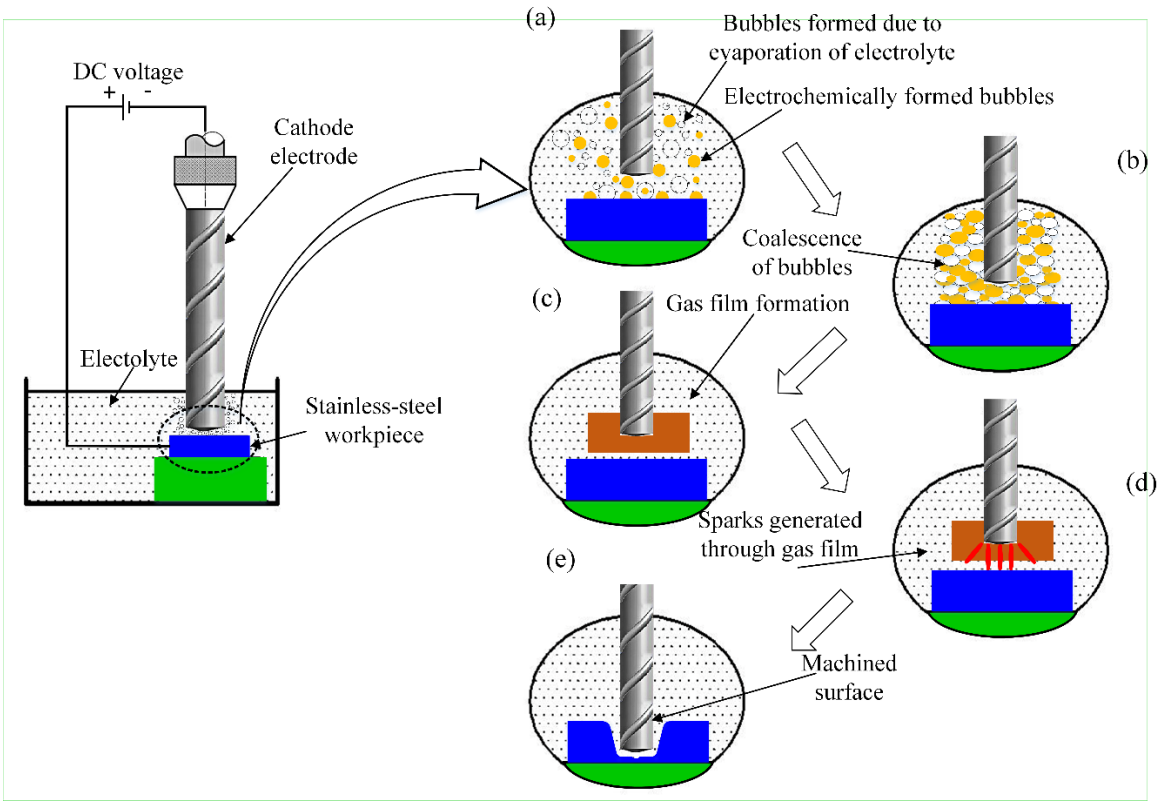

Figure 1. Schematic diagram of the ECDD principle: (a) bubble generation, (b) accumulation of bubbles, (c) gas film formation, (d) the electric spark generated, (e) thermally etched micro-pit.

Xu et al. developed an observation system integrated with a PC device and charge-coupled device (CDD). The state of the machining gap was observed by a CDD observation system. The observed results

showed that the machining phenomenon was different at the machining gap (including the frontal gap and the lateral gap) [27]. For this reason, the mechanism of material removal is different for the practical machining process. Fig 2 illustrates, in detail, the mechanism of material removal in the ECDD process using a high-speed rotating helical tool-electrode. In this micro-pit drilling process, at the frontal gap, the tungsten carbide helical tool-electrode feeds toward the work-piece. As the machining distance between the end face of the tungsten carbide helical tool-electrode and the surface of the work-piece becomes smaller than the discharge gap, removal of the work-piece material is mainly caused by high-temperature corrosion due to the electric spark discharge phenomenon. Moreover, because the electrolyte is tap water with extremely low conductivity, electrochemical dissolution simultaneously occurs in the frontal gap of the tool-electrode. Thus, during the process of material removal, electrochemical dissolution merely plays a secondary role.

In the lateral gap, the material removal mechanism is different from that in the frontal gap. The machining distance of the side gap between the tungsten carbide helical tool-electrode and the sidewall of the micro-pit is increased by the synergy of electrochemical corrosion and electric spark discharge. In the lateral gap, the electric spark discharge phenomenon is gradually decreased. When the lateral machining gap exceeds the critical maximum value, electric spark discharge erosion is completely suspended. Consequently, in the lateral machining gap, electric spark discharge erosion occurs exclusively by electrochemical dissolution. Thus, the rough surface quality is machined by the EDM, and a better surface quality is obtained by this ECM process.

In summary, this hybrid machining process can be referred to as the ECDM process. In the practical ECDM process, at the frontal gap between the tool-electrode and the work-piece surface, the EDM process plays a dominant role in the removal of the work-piece material. The expansion of the micro-pit at the lateral gap mainly depends on the ECM process. In the frontal gap, the EDM process continuously occurs. While in the lateral gap, the mechanism for material removal is gradually shifted from EDM machining to ECM processing. Eventually, in the lateral gap, material removal is entirely by ECM processing.

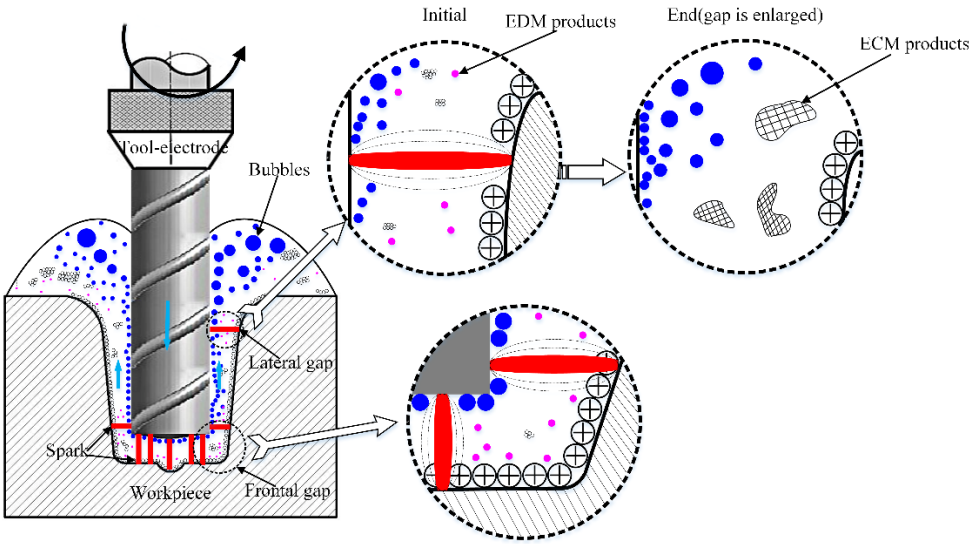

Figure 2. Mechanism of material removal in the ECDD process with a high-speed rotating helical tool-electrode

3. EXPERIMENTAL SET-UP AND PROCEDURES

In this paper, many experiments are presented that investigate the material removal mechanism during the practical ECDM process. This machining process uses a high-speed rotating tungsten carbide helical tool-electrode. Fig 3 shows a schematic diagram of the experimental set-up, which consisted of a motion platform, motorized spindle, high-speed camera, electrolytic tank, fixed resistance (1Ω), oscilloscope, motion controller, frequency converters, monitoring interface, and high frequency pulse power. Among these, the oscilloscope was used to collect the machining current signal during the machining process, and the high-speed camera was employed to observe the phenomenon of bubble generation, gas film formation and electric spark generation through the gas film.

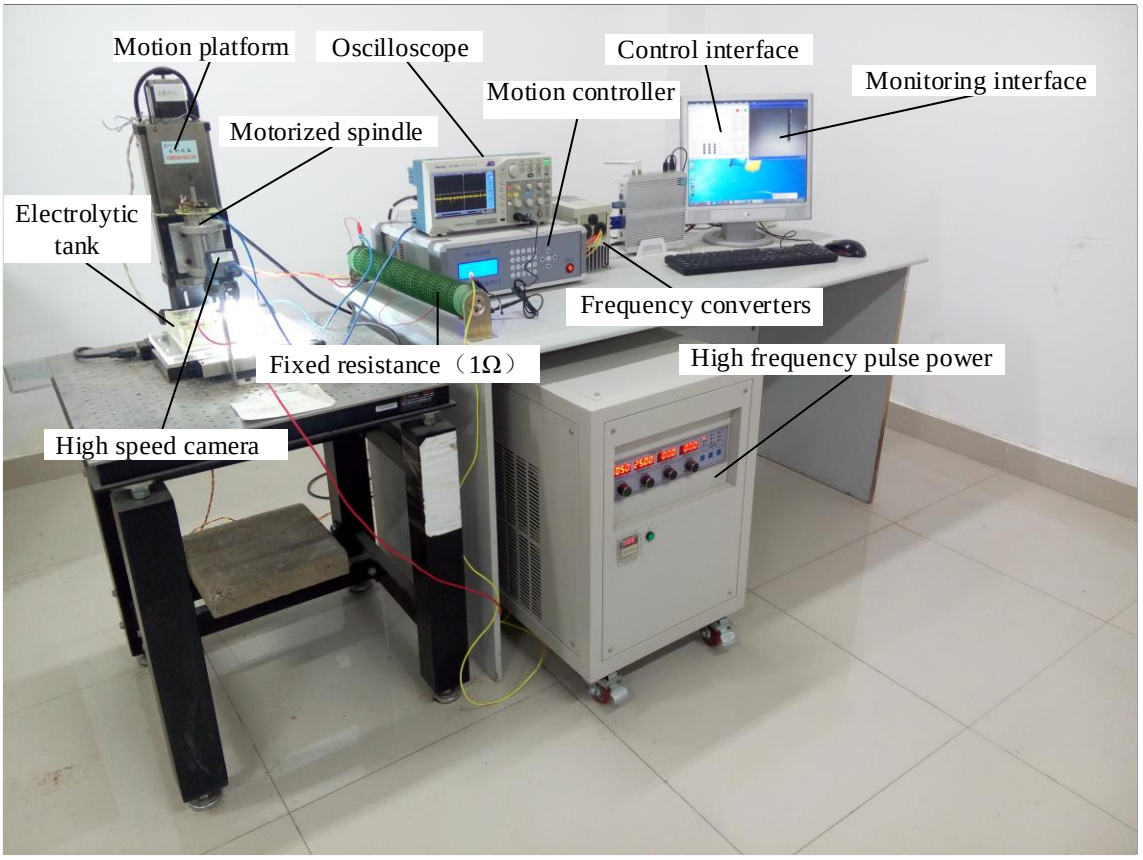

Figure 3. Schematic diagram of the experimental set-up

The experimental parameters for the ECDD process are as shown in Table 1. In the experiments, the work-piece material is ANSI 304 stainless steel, the applied voltage is 10 V, the frequency of the applied voltage is 25 kHz, the tungsten carbide helical tool-electrode is used as the tool-electrode, the tool-electrode diameter is 250 μm, the duty is 50%, the feed rate of the tool-electrode is 1 μm/s, the initial machining gap is 40 μm, the machining time is 100 s, and the electrolyte is tap water. The tool-electrode rotational speed range from 3,600 rpm to 18,000 rpm is selected for the experiment, and the

effect of tool-electrode rotational speed on the gas film formation and the machining current is studied at different tool-electrode rotational speeds.

Table 1. Experimental parameters

Item	Value
Applied voltage	10 V
Initial machining gap	40 μm
Frequency	25 kHz
Duty factor	50%
Feed rate	1 μm/s
Tool-electrode	Tungsten carbide helical electrode
Tool-electrode rotational speed	3600 rpm, 9000 rpm, 10800 rpm, 14400 rpm, 18000 rpm
Tool-electrode diameter	250 μm
Electrolyte	tap water
Work-piece	stainless steel (ANSI 304)

4. RESULTS AND DISCUSSION

A series of experiments were conducted with different rotational speeds by the ECDD set-up. The effects of the different tool-electrode rotational speeds on the material removal mechanism of the work-piece are discussed, and the other machining parameters remain unchanged.

4.1 Effect of the tool-electrode motion state on the discharge phenomenon

Tang et al. reported that gas film evolution in electrochemical discharge machining process. The gas film is crucial in both spark generation and machining process. Thus, the mechanism of gas film evolution and the status of gas film need to be further studied [29,30]. The effect of the helical tool-electrode motion state on the spark discharge phenomenon in the ECDM process is illustrated in Fig 4. When the tool-electrode is in a stationary state, with the help of the high-speed camera, it is observed that a small number of bubbles are generated on the surface of the tool-electrode, as shown in Fig 4(a). As electrochemical electrolysis progresses, the number of bubbles generated on the surface of the tool-electrode increase. Subsequently, these bubbles coalesce to form a gas film around the surface of the tool-electrode. However, under the above conditions, the surface of the gas film appears to be turbulent, as shown in Fig 4(b) (yellow area). As the experiment continues, the electrochemical corrosion rate on the surface of the work-piece is increases. In this case, the work-piece material is mainly removed by electrochemical corrosion, and no electric spark discharge phenomenon occurs during the whole machining process.

When the tool-electrode is in a rotational state, the electrochemical electrolysis reaction first occurs on the surface of the tool-electrode. The anode (work-piece) is slightly dissolved in the

electrolyte, and bubbles are generated on the surface of the tool-electrode (cathode). Simultaneously, centrifugal force is generated due to the high-speed rotation of the tool-electrode. Under this centrifugal force, the gas-liquid separation ability is enhanced. Bubbles begin to accumulate on the surface of the tool-electrode to form a denser insulating film, as shown in Fig 4(c) (yellow area). When the applied machining voltage reaches the critical machining voltage, the insulating film is broken-down. Eventually, at the end of the tool-electrode, the electric spark discharge phenomenon is generated, as shown in Fig 4(d) (red area).

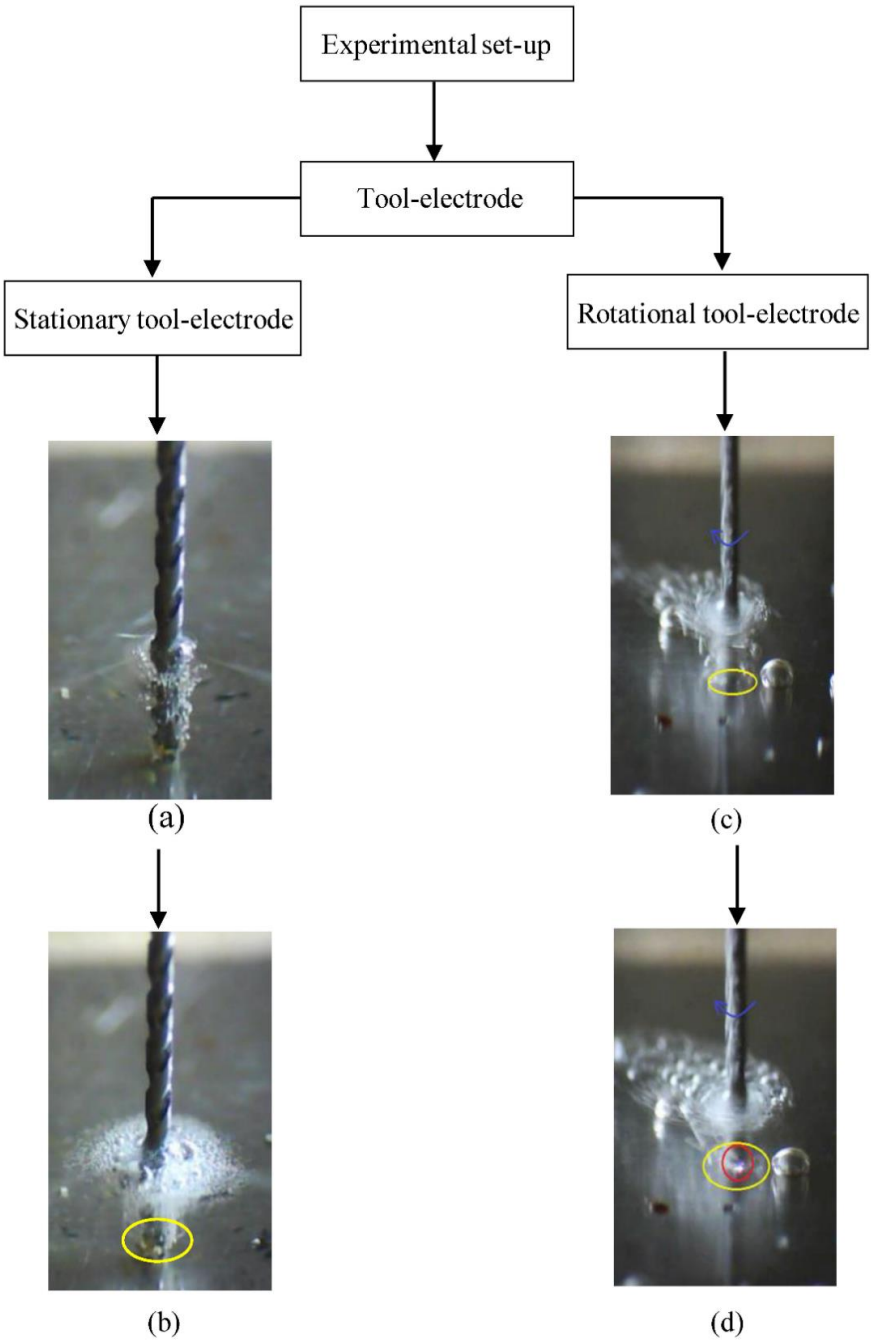

Figure 4. Effect of the tool-electrode motion state on the electric spark discharge phenomenon

4.2 Effect of the tool electrode rotational speed on the discharge phenomenon

Jiang et al. established a machining process modelling of ECDM, including the spark generation and the work-piece material removal. By comparing the simulation analysis with the experimental results, we can draw that the material removal of work-piece due to thermal melting and chemical etching [28]. Fig 5 shows the effect of different tool-electrode rotational speeds on the electric discharge phenomenon. As seen, under different rotational speed, the generation of bubbles, the coalescence of bubbles, the formation of a gas film and the electric discharge phenomenon are different. When the rotational speed of the tool-electrode reaches 3,600 rpm to 9,000 rpm, the bubbles still slightly drift. As a result, the quality of the gas film formed in this way is not uniform, and it is unstable. Therefore, at the end of the tool-electrode, the electric discharge phenomenon is not obvious. When the rotational speed of the tool-electrode reaches from 10,800 rpm to 14,400 rpm, the bubbles have almost no drift. At the end of the tool-electrode, the electric discharge phenomenon is obvious. As the rotational speed of the tool-electrode is further increased to 18,000 rpm, the gas film formed on the surface of the tool-electrode becomes more uniform and more stable. Finally, at the end of tool-electrode, the electric discharge phenomenon becomes brighter.

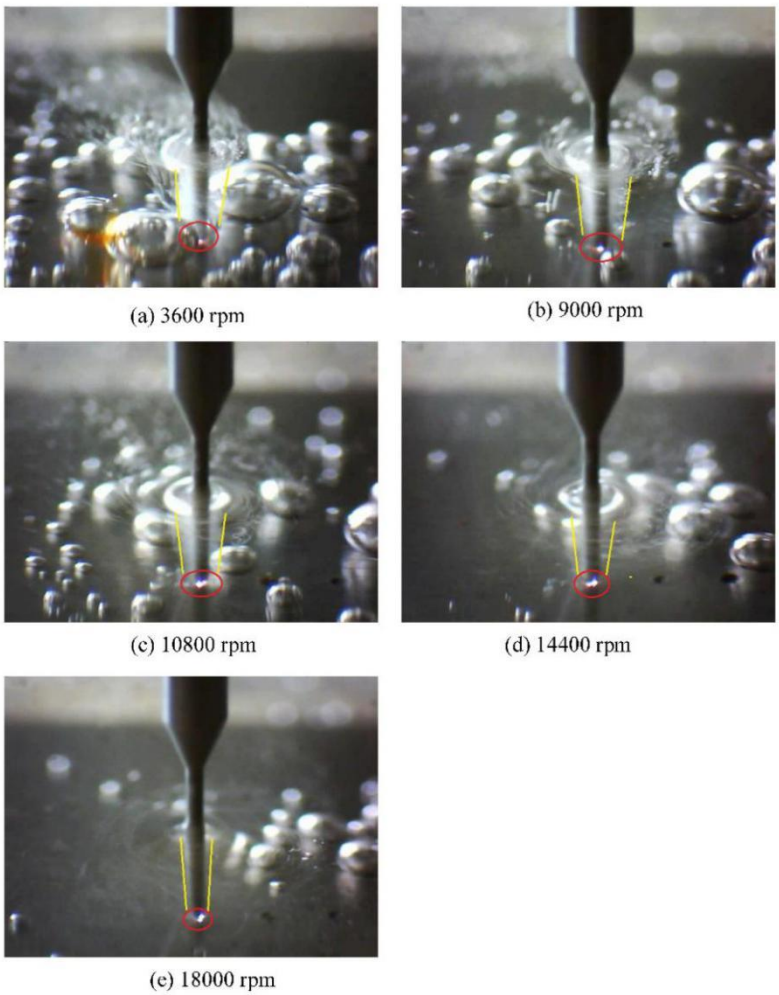

Figure 5. Phenomenon of electric spark discharge with different tool-electrode rotational speeds

4.3 Effect of the tool-electrode rotational speed on the machining current

During the ECDD practical machining process, the machining current is an important parameter. The current signal waveform during the electrochemical discharge drilling process is shown in Fig 6. In the initial stage, electrochemical electrolysis occurs on the surface of the tool-electrode and generates a large number of bubbles. Under centrifugal force, these bubbles adhere to the surface of the tool-electrode and form a dense gas film. The gas film is equivalent to the insulating layer, which results in an increase in the resistance of the machining gap. Thus, the machining current in the processing circuit is very small (close to 0 A), corresponding to the A-B section shown in Fig 6. When the potential difference between the lower end of the tool-electrode and the upper surface of the work-piece increases to the critical machining voltage, the insulating gas film is instantaneously broken-down. As a result, the resistance becomes instantaneously small and the current in the machining circuit instantaneously increases, corresponding to the B-C section shown in Fig. 6. At the same time, the electric discharge phenomenon is generated on the end surface of the tool-electrode. Since the discharge time is very short, the bubbles generated by the electrochemical electrolysis reaction quickly adhere to the surface of the tool-electrode and form an insulating gas film. Thus, the resistance in the machining gap instantaneously increases, causing the machining current in the processing circuit to begin to decrease again, corresponding to the C-D-E section shown in Fig. 6.

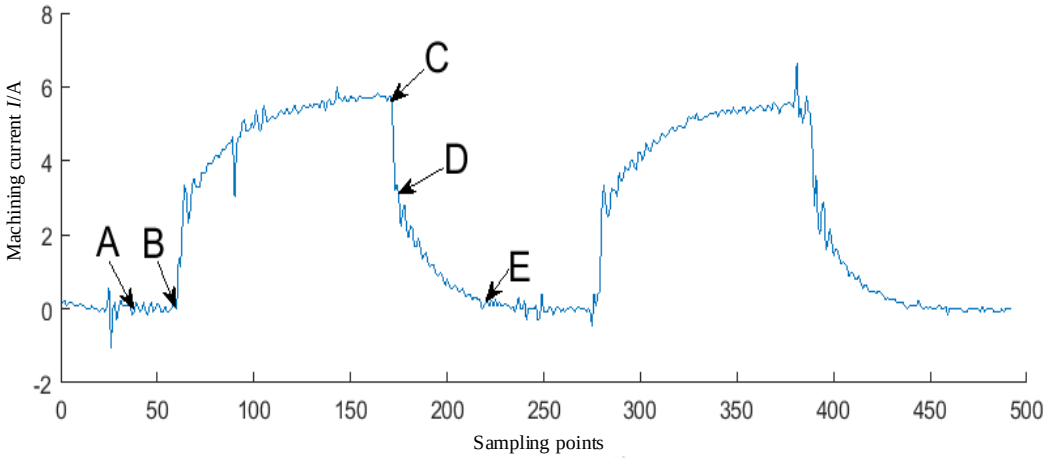

Figure 6. Current signal waveform during the machining process

Liu et al. developed wire electrochemical discharge machining (WECDM) with a rotating helical wire-tool electrode. They also studied the effect of the spindle speed on the machining current signals and found that the peak machining current increases at higher rotational speeds [25]. In this ECDD process, the effect of the tool-electrode rotational speed on the machining current is different, as shown in Fig 7. As the rotational speed of the tool-electrode increases, the peak value of the machining current gradually increases during the machining process. The possible reason for this increase could be because centrifugal force gradually increases as the rotational speed of tool-electrode increases. As a result, the ability to accumulate bubbles on the surface of the tool-electrode is enhanced. Thus, the active contact

area of the gas film attached to the end surface of the tool-electrode increases and the gas film becomes denser. The voltage required for the break-down of the insulating film is also increased. In general, the peak value of the machining current signal increases with the increase in the tool-electrode rotational speed over a certain range.

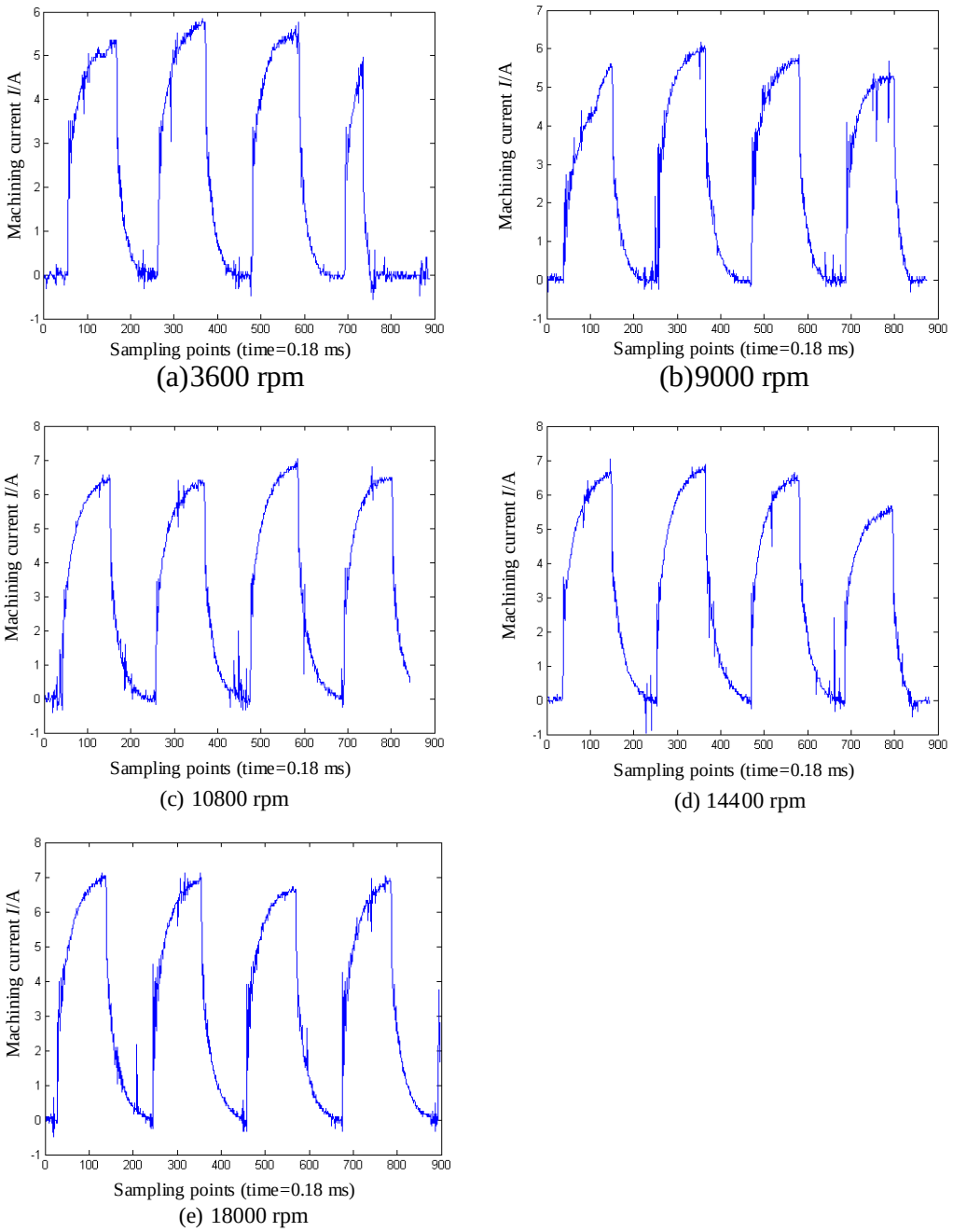

Figure 7. Effect of the tool-electrode rotational speed on the machining current

To further investigate the influence of the tool-electrode rotational speed on the machining current signal, the machining current signal at different rotational speeds is statistically analysed. The total discharge times of a peak machining current greater than 4 A are counted during the machining

period. The range of the peak machining current is divided into three parts: 4 A ≤ I < 5 A, 5 A ≤ I < 6 A, and 6 A ≤ I < 10 A.

The relationship between the peak value distribution of machining current and the tool-electrode different rotational speed is shown in Fig 8. The peak machining current of 6 A≤ I <10 A increases with the increase in the tool-electrode rotational speed, and the percentage is also significantly increased. However, the peak machining current of 4 A ≤ I < 5 A and 5 A ≤ I < 6 A decreases with the increase in the tool-electrode rotational speed, and the percentage is also significantly decreased.

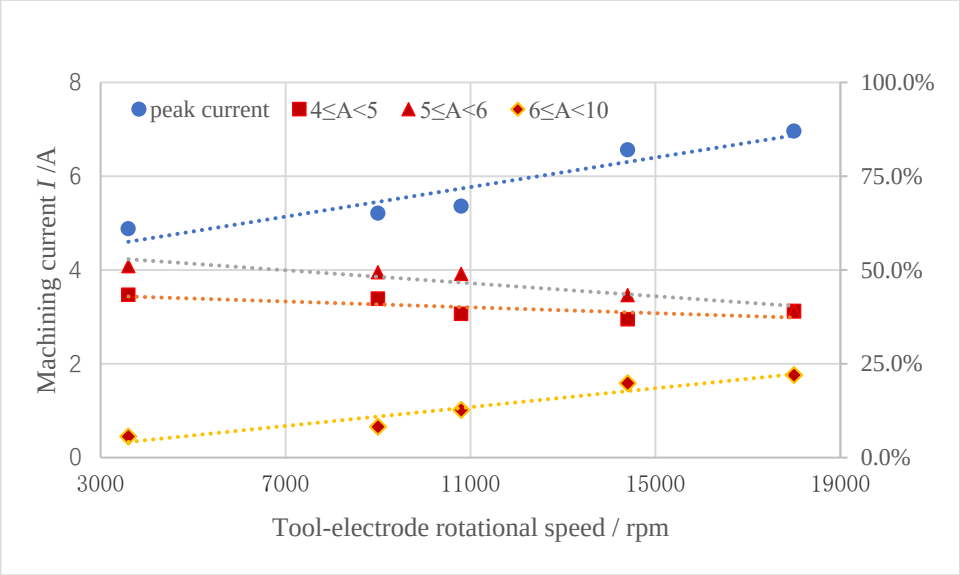

Figure 8. Relationship between the peak value distribution of the machining current and the different tool-electrode rotational speeds

4.4 Effect of the tool-electrode rotational speed on the micro-pit diameter

In the ECDD process, the effect of the tool-electrode rotational speed on the micro-pit diameter is different, as shown in Fig 9. Liu et al. demonstrated the effect of the spindle speed on the diameter of the micro-holes in the WECDM process, with the other machining parameters remaining unchanged. They observed that the standard deviation values of the diameter of micro-holes increase as the tool-electrode rotational speed increases. In addition, during their experiment process, the range of the spindle speed was from 3,000-12,000 rpm [25]. Therefore, it is necessary to study the effects of a higher rotational speed of the tool-electrode on the diameter of micro-pits. As the tool-electrode rotational speed gradually increases, the diameter of the micro-holes also increases. The reason for this phenomenon may be that as the rotational speed of tool-electrode increases, the centrifugal force generated on the surface of tool-electrode increases. As a result, the ability of the tool-electrode surface to accumulate bubbles is enhanced. Subsequently, a gas film is formed on the surface of the tool-electrode. Since the quality of the formed gas film is also relatively good, it is easy to generate a spark discharge in the machining gap. Within a certain machining period, the spark discharge time is increased. Therefore, the diameter of the micro-pits increases with the increase in the tool-electrode rotational speed over a certain range.

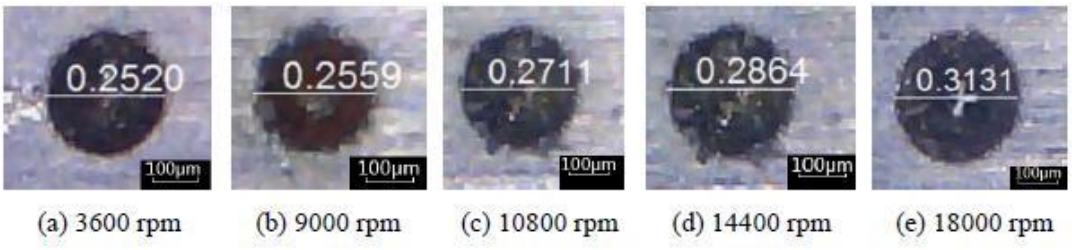

Figure 9. Effect of the tool-electrode rotational speed on the micro-pit diameter

The reaming ratio of t is defined as:

$$t = \frac{d - d_0}{d} \quad (1)$$

In the definition of formula (1), t is the reaming ratio, d is the measured value of the micro-pit diameter, and d_0 is the theoretical value of the micro-pit diameter.

The relationships among the micro-pit diameter, the reaming ratio and the tool-electrode rotational speed are shown in Fig 10. As seen, the micro-hole diameter gradually increases with the increase in the tool-electrode rotational speed over a certain range, and the reaming ratio of t also increases.

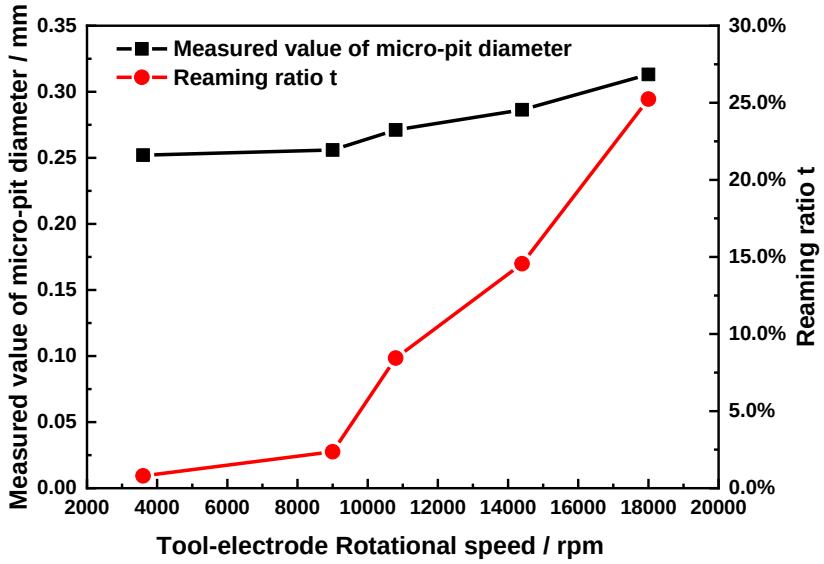

Figure 10. Relationships among the micro-pit diameter, the reaming ratio and the tool-electrode rotational speed

4.5 Effect of the tool-electrode rotational speed on the depth of micro-pits

Xu et al. presented a hybrid electrochemical discharge drilling process with a metal tube electrode. By this machining process, they eventually fabricated a series of small deep holes with depth of 4 mm and diameter of 0.5 mm [27]. The depth of micro-pits can be measured by the PS50 type three-

dimensional surface morphology instrument, and the three-dimensional surface morphology of micro-pits can be scanned by this equipment. Subsequently, the scanned three-dimensional surface topography of micro-pits can be cut-open. Thereby, the cross-sectional depth of micro-pits can be obtained, as shown in Fig 11. As seen, the cross-sectional depth of micro-pits gradually increases with the increase in the tool-electrode rotational speed during the same machining time. The possible reason for this result is that the total discharge times gradually increase with the increase in tool-electrode rotational speed over the same machining period.

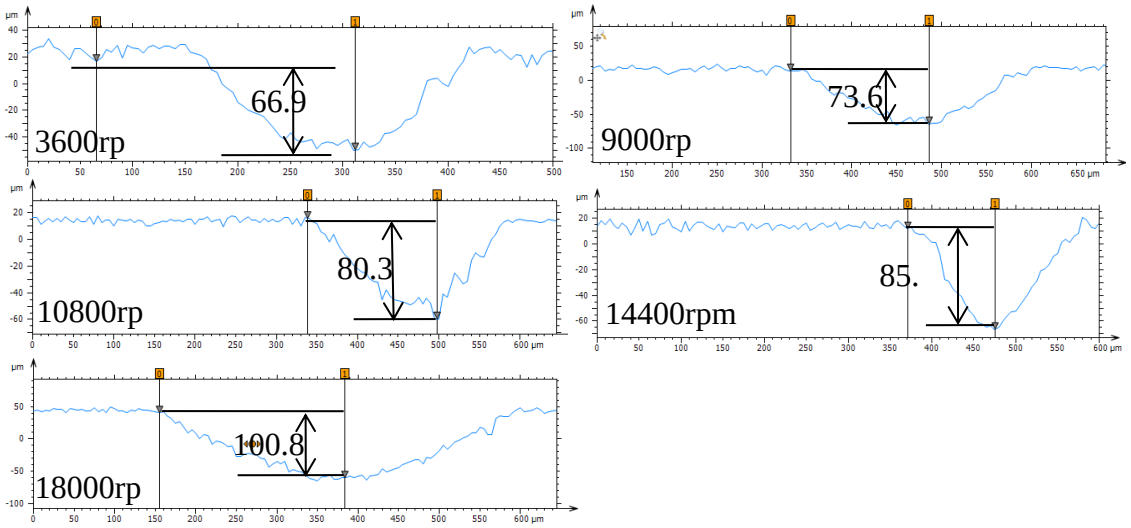

Figure 11. Relationships among the cross-sectional depth of the micro-pit and the different tool-electrode rotational speeds

In this experiment, because the machining time is the same, the material removal rate of the work-piece material can be estimated by measuring the volume of the micro-pits. The relationship between the volume of the micro-pits and the tool-electrode rotational speed is shown in Fig 12. As seen, the volume of the micro-pits gradually increases with the increase in the tool-electrode rotational speed over certain range. That is, the material removal rate of the work-piece material increases with the increase in the tool-electrode rotational speed. Thus, over certain range, the increase of the tool-electrode rotational speed can increase the material removal rate of the work-piece material.

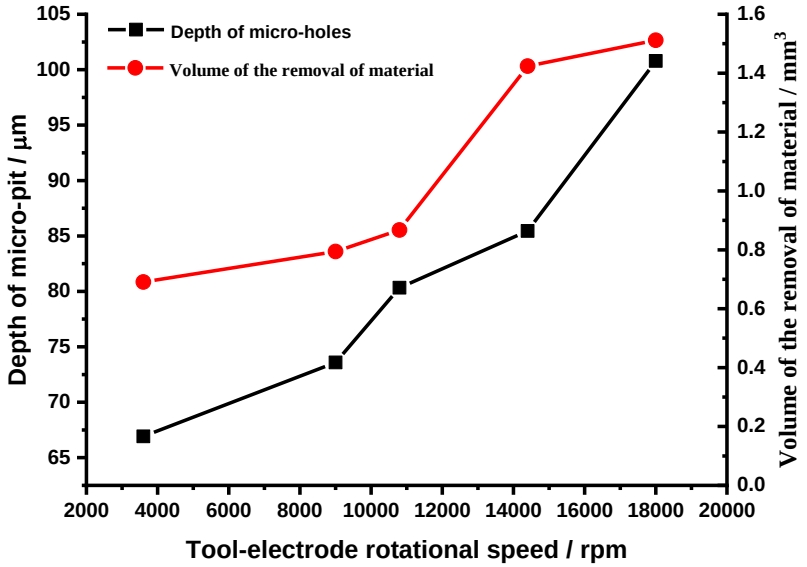

Figure 12. Relationship between the volume of the micro-pit and the tool-electrode rotational speed

5. CONCLUSIONS

In this paper, an experimental investigation of the removal mechanism of work-piece material during the practical ECDD process is presented. The experimental set-up for the ECDD process using a high-speed rotating tungsten carbide helical tool-electrode is presented. Subsequently, many experiments were conducted to study the influence of the different tool-electrode rotational speeds on the removal mechanism. The effects of the different tool-electrode rotational speeds on the bubble generation, the formation of gas film, the electric spark discharge phenomenon, the machining current, and the material removal rate are discussed. Finally, we draw the following conclusions from the analysis of the experimental results:

1. It is observed that the machining peak current signal increases with the increase of the tool-electrode rotational speed within a certain range.

2. It is observed that the electric spark discharge phenomenon is enhanced with the increase of the tool-electrode rotational speed within a certain range.

3. During the machining process, the depth of the machined micro-pits increases with the increase in the tool-electrode rotational speed within a certain range. Simultaneously, the material removal rate is enhanced.

4. During the machining process, as the rotational speed of the tool electrode increases, the ability of bubbles to accumulate on the surface of the tool-electrode is enhanced with the increase of the tool-electrode rotational speed within a certain range. Thus, under this condition, a denser insulating gas film is more easily formed on the surface of the tool-electrode.

5. During the machining process, the motion state of the tool-electrode directly affects the generation of the electric spark discharge phenomenon. When the tool-electrode is stationary, the electric spark discharge phenomenon does not occur in the machining gap. When the tool-electrode is in a high-

speed rotational state and the machining voltage reaches the critical machining voltage, the electric spark discharge phenomenon occurs.

ACKNOWLEDGMENTS
This research is supported by the National Natural Science Foundation of China (Grant No. 51705002), and the Provincial Natural Science Foundation of Anhui (Grant No. 1608085 ME89).

References

1. J.W. Judy, *Smart Mater. Struct.*, 10 (2001) 1115.
2. D. Sarvela, *MEMS J.*, 2010.
3. X.Y. Chen, Z.Y. Wu, *Microsyst. Technol.*, 23 (2017) 4319.
4. M. Singh, S. Singh, *Adv. Manuf. Mater. Sci.*, (2018) 139.
5. B. Bhattacharyya, B.N. Doloi, S.K. Sorkhel, *J. Mater. Process. Technol.*, 95 (1999): 145.
6. P. Antil, S. Singh, A. Manna, *Iranian J. Sci. Technol.*, 2019.
7. Y. Liu, C. Zhang, S.S. Li, C.S. Guo, Z.Y. Wei, *Processes*, 7 (2019) 195.
8. M. Singh, S. Singh, *Proc. Inst. Mech. Eng.*, 233(2019) 1425.
9. H. Kurafuji, K. Suda, *Ann. CIRP*, 16 (1968) 415.
10. N.H. Cook, G.B. Foote, P. Jordan, B.N. Kalyani, *J. Eng. Ind.,* 95 (1973) 945.
11. S. Tandon, V.K. Jain, P. Kumar, K.P. Rajurkar, *Precis. Eng.*, 12 (1990) 227.
12. R. Wüthrich, V. Fascio, *Int. J. Mach. Tools Manuf.*, 45 (2005) 1095.
13. H.H. Langen, V. Fascio, R. Wüthrich, D. Viquerat, *Microrob. Microassem. III*, 4568 (2001) 304.
14. X.D. Cao, B.H. Kim, C.N. Chu, *Int. J. Precis. Eng. Manuf.,* 14 (2012) 5.
15. K.H. Nguyen, P.A. Lee, B.H. Kim, *Int. J. Precis. Eng. Manuf.*, 16 (2015) 5-12.
16. C.K. Yang, C.P. Cheng, C.C. Mai, A.C. Wang, J.C. Hung, B.H. Yan, *Int. J. Mach. Tools Manuf.,* 50 (2010) 1088.
17. C.K. Yang, K.L. Wu, J.C. Hung, S.M. Lee, J.C. Lin, B.H. Yan, *Int. J. Mach. Tools Manuf.,* 51 (2011) 528.
18. I. Basak, A. Ghosh, *J. Mater. Process. Technol.,* 62 (1996) 46.
19. C.T. Yang, S.S. Ho, B.H. Yan, *Key Eng. Mater.*, 196 (2001) 149-166.
20. Z.P. Zheng, K.L. Wu, Y.S. Hsu, F.Y. Huang, B.H. Yan, *Proc. AEMS07*, (2007)28.
21. N. Gautam, V.K. Jain, *Int. J. Mach. Tools Manuf.,* 38 (1998) 15.
22. S.F. Huang, D. Zhu, Y.B. Zeng, W. Wang, Y. Liu, *Adv. Mater. Res.,* 295 (2011) 1794.
23. S.F. Huang, Y. Liu, J. Li, H.X. Hu, L.Y. Sun, *Mater. Manuf. Processes,* 29 (2014) 634.
24. X.L. Fang, P.F. Zhang, Y.B. Zeng, N.S. Qu, D. Zhu, *J. Mater. Process. Technol.,* 227 (2016) 129.
25. Y. Liu, Z.Y. Wei, M.Y. Wang, J.H. Zhang, *J. Manuf. Processes,* 29 (2017) 265.
26. Y. Zhang, Z.Y. Xu, D. Zhu, *J. Xing, Int. J. Mach. Tools Manuf.,* 92 (2015) 10.
27. Z.Y. Xu, Y. Zhang, F. Ding, F. Wang, *Int. J. Adv. Manuf. Tech.,* 95(2018) 3037-3044.
28. B.Y. Jiang, S.H. Lan, J. Ni, Z.Y. Zhang, *J. Mater. Process. Tech.*, 4(2014) 892.
29. W.D. Tang, X.M. Kang, W.S. Zhao, *Int. J. Electrochem. Sci.*, 14(2019) 970.
30. W.D. Tang, X.M. Kang, W.S. Zhao, *J. Micromech. Microeng.*, 27(2017) 065013.